ISIJ International, Vol. 38 (1998), No. 11, pp. 1153–1164

Review

Effects of Rare Earth Element on Isothermal and Martensitic Transformations in Low Carbon Steels

T. Y. HSU (XU Zuyao)

School of Materials Science and Engineering, Shanghai Jiao Tong University, Shanghai 200030, China.

(*Received on May 22, 1998; accepted in final form on June 26, 1998*)

Rare earth elements (RE) may segregate at the grain boundaries of austenite, lead to form carbide and refine the austenite grain. In case of no change of grain size and carbon content of austenite, an addition of RE is beneficial to the hardenability of steels. In case of a marked refinement of austenite grain, addition of RE will deteriorate the hardenability. The incubation period of the proeutectoid ferrite can be expressed as a function of grain boundary energy, grain size, activation energy for growth and the driving force for transformation and the calculated results are in good agreement with the experimental data. RE may retard the isothermal pearlitic transformation, because RE diminishes the diffusion coefficient of carbon as well as tends to segregate at Fe_3C/α interface, showing a pinning effect on the transformation. RE reduces the lamella spacing of the pearlite owning to lowering the interfacial energy, *e.g.*, from 0.7 to 0.53 J/m^2 in 0.27C–1Cr–RE steel. RE tends to segregate at ferrite/island interface in the granular bainite. In grain refined steel, at the earlier stage of bainite formation, the transformation rate is high while at later stage it becomes sluggish. The activation energies of pearlitic and bainitic transformations increase by the addition of RE. The segregation of RE at ferrite/island interface may act as a drag effect. A drag factor α is expressed as a function of transformation fraction and calculated in a 0.27–1Cr–RE steel. RE segregates at the grain boundary of austenite and this kind of distribution will not be changed during the martensitic transformation. It is reasonable to predict that RE will lower the martensite/austenite interface energy, resulting in the formation of a finer lath structure. RE lowers M_s, decreases the amount of the retained austenite and retards the autotempering process. It is emphasized that the amount of the retained austenite, γ, in quenched low carbon steel depends on not only the M_s and the temperature of quenching medium, T_q, but also the influence of alloying elements on the carbon diffusion during quenching. A general equation modified from the Magee's equation is derived as $\gamma=\exp\{\alpha(C_1-C_0)-\beta(M_s-T_q)\}$ where C_0 and C_1 are carbon concentrations in austenite before and after quenching respectively, α and β are constants. RE decreases M_s but also lowers C_1 so as to reduce the amount of the retained austenite.

KEY WORDS: hardenability; proeutectoid ferrites; pearlitic transformation; bainitic reaction; martensitic transformation; retained austenite; rare earth; low carbon steel.

1. Introduction

It is well known that the rate earth metals (RE) are beneficial for cleaning of steel. Works concerning the effect of RE on phase transformations in steel are rather few and the results are controversial and in confusion.[1,2] These may be resulted from the following factors: (1) different experimental conditions, such as the different cooling rate used in continuous cooling for the study of phase transformations and (2) different methods of feeding the RE into steel, causing various state of RE existing in steel, *e.g.*, forming compounds such as sulfides, carbides and oxides and dissolving in austenite. The solubility of RE in iron is very limited.[3–5] For example, the solubility of Ce in steel matrix does not exceed 0.05 wt%, as determined by isotope Ce measurement.[4] **Figure 1** shows the RE content in solid solution and intermetallic phases as a function of the total RE content in a 0.25C–Mn–Ti–B steel.[5]

It has been well found that RE may segregate on the grain boundary of austenite[3,6,7] and ferrite[8,9] as well as to the Fe_3C/α interface in pearlite and at island interfaces in bainite.[10,11]

From Fig. 1, one can recognize that as the amount of RE addition in steel is about 0.05–0.1 wt%, most of the RE is in the form of inclusions and the dissolved amount in solid solution is very small.

Owing to the much larger atomic radius of RE, *e.g.*, 0.3745 and 0.3637 nm for β-La and β-Ce respectively, than that of α-Fe (0.254 nm), not only the solubility of RE in iron is very limited but also the RE tends to segregate on grain boundary or interface between phases in iron based alloys. **Figure 2** shows the segregation of Ce on the austenite grain boundary in a Mn–V steel containing 0.15% Ce, 0.007% S and 0.02% P.[2] In a Fe–0.1% Ce alloy, the concentration of Ce, on grain boundary of α Fe, 1.5% Ce, is 20 folds higher than that in the matrix.[3]

Table 1 shows the segregation of La on Fe_3C/α interface of pearlite formed isothermally at 730°C in a 0.2C–1Mn steel.[10,11] **Tables 2** and **3** show the segregation of RE on proeutectoid ferrite boundaries, at Fe_3C/α interface in pearlite as well as island boundaries of bainite in a 0.27C–1Cr steel containing 0.17RE.[10,11]

The segregation of RE on grain boundaries as well as at interphase boundaries in steel may lower the boundary energy and affect the nucleation and growth in phase transformations. Rare earth atoms are strong carbide forming elements. As part of the RE addition combines carbon to form carbide, the carbon content in austenite may be reduced. If the carbide exists at the austenite grain boundaries, they will hinder the grain growth. The lowering of the grain boundary energy in steel containing RE would reduce the driving force for the movement of the boundary, and there may be the drag effect as the carbide formed on the grain boundary. In addition, the RE may decrease the diffusivity of carbon. Accordinly, RE may refine the austenite grain, for example, the austenite grain size of the specimen after austenitization at 900°C for 10 min is ASTM No. 6 in 0.2C–1Mn steel, while it will be ASTM No. 8 in 0.2C–1Mn–RE.[12] The variation of austenite grain size will in turn affect the hardenability and transformation characteristics in steels.

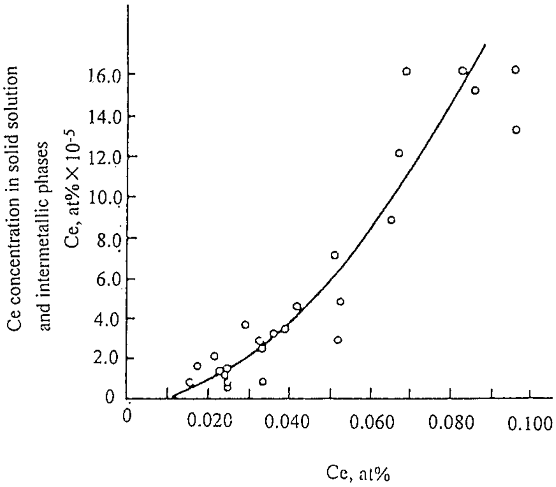

Fig. 1. Concentration of Ce in solid solution and in intermetallic phases as a function of the total content in a 0.25C–Mn–Ti–B steel.[5]

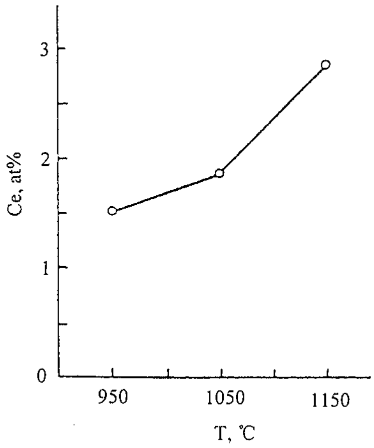

Fig. 2. Concentration of Ce at austenite grain boundaries in Mn–V steel containing 0.15% Ce and 0.02% S quenched from various temperature.[2]

This paper attempts to review the effect of rare earth elements (RE) on isothermal transformations including isothermal proeutectoid ferrite formation related to the hardenability of steel, pearlitic and bainitic kinetics and morphology as well as the martensitic transformation in low carbon steels. Here, the term low carbon steel refers to the steel showing lath martensite in microstructure after quenching, but not the restricted range of the carbon content in steels. The different effects of RE on some transformations, especially on the hardenability of steel will be shown under different states of RE existing in structures, *i.e.*, (1) RE dissolved in the solid solution and does not affect the austenite grain size remarkably, and (2) RE partly dissolved in the solid solution and partly formed compound such as carbide. Discussion and critical review on various experimental results are given.

2. Effect of RE on the Hardenability and TTT Diagram of Steel

Guliaev and Ulianin in previous USSR reported that RE increases the hardenability of a 0.4C–1Cr steel.[13] Opposite results about the effect of RE on hardenability of steel also appeared,[3] for example, an addition of

Table 1. Distribution of RE (wt%/at%) in pro-eutectoid ferrite and pearlite isothermally formed at 730°C in a 0.2C–1Mn–RE steel and in a 0.27C–1Cr–RE (wt%/at%) steel.[10]

Rare earth element	Pro-eutectoid α boundary	Pearlite Fe_3C	Pearlite Fe_3C/α
La	0.00/0.00	0.00/0.00	0.16/0.06
Ce	0.00/0.00	0.00/0.00	0.00/0.06

Table 2. Distribution of RE (wt%/at%) in pro-eutectoid ferrite and pearlite isothermally formed at 730°C in a 0.27C–1Cr—RE steel.[10]

Position No.	Rare earth element	Pro-eutectoid α boundary	Pro-eutectoid α within grain	Pearlite Fe_3C	Pearlite α	Pearlite Fe_3C/α
1	La	0.10/0.04	0.00/0.00	0.20/0.07	0.30/0.12	0.70/0.28
	Ce	0.00/0.00	0.00/0.00	0.08/0.03	0.36/0.14	0.53/0.21
2	La	0.00/0.00	0.00/0.00	0.21/0.08	0.46/0.18	0.36/0.14
	Ce	0.00/0.00	0.02/0.01	0.15/0.06	0.52/0.21	0.24/0.10
3	La	0.04/0.01	0.00/0.00	0.00/0.00	0.00/0.00	0.50/0.20
	Ce	0.01/0.00	0.00/0.00	0.00/0.00	0.00/0.00	0.25/0.10
4	La	0.00/0.00	0.02/0.01	0.00/0.00	0.09/0.04	0.08/0.03
	Ce	0.00/0.00	0.00/0.00	0.00/0.00	0.00/0.00	0.24/0.09

0.1–0.4% RE in a 0.25C–Mn–Ti–V steel, quenched from 850°C, has shown the detrimental effect on the hardenability and it was suggested that the segregation of RE on the austenite grain boundary would reject B which must enhance the hardenability.[14)]

In the case of unchange of the austenite grain size, the addition of RE will increase the hardenability of steel as shown in **Fig. 3** for steels 1 and 2 of which the composition and grain size are shown in **Table 4**.[15)]

By the addition of 0.11 wt% Ce in a 0.12C–1.35Si–1.18Mn–0.004S–0.018P steel, the austenite grain size at 1 000°C for 10 min changes from ASTM No. 9 to No. 10 and the CCT curve moves toward right-side, resulting in the formation of 50% ferrite and granular bainite, *i.e.*, the amount of ferrite and bainite is 5% greater than that of steel without Ce.[16)]

In case of considerable refinement of the austenite grain size and formation of RE carbide with high melting point resulted from the addition of RE, the hardenability of steel should be lowered by the addition of RE, as shown in **Fig. 4**, the TTT diagram of the steels 3 and 4 (Table 4)[17)] and in **Fig. 5**, that of the steels 5–8 (Table 4),[12)] implying that under such case, the grain refinement acts as an important role controlling the nucleation of proeutectoid ferrite and the hardenability of the steel.

As RE segregates at the grain boundary of austenite and lowers the grain boundary energy, RE may be beneficial to the hardenability of steel. However, as RE forms carbides with high melting point, refines the austenite grain or increases the nucleation site of proeutectoid ferrite and bainite as well as reduces the carbon content in austenite, RE may deteriorate the hardenability of steel. Finear grain of austenite may result in a larger transformation rate of $\gamma \rightarrow \alpha$ at early-stage. RE reduces the diffusion coefficient of carbon and RE-carbides may hinder the Fe_3C/α interface migration by pinning effect and may retard the rate of transformations $\gamma \rightarrow \alpha$ and $\gamma \rightarrow \alpha + Fe_3C$.

Table 3. Distribution of RE (wt%/at%) in granular bainite isothermally formed at 450°C in a 0.27C–1Cr–RE steel.[10)]

Position No.	Rare earth element	Bainite within island	Bainite boundary of island	Bainite boundary of ferrite	Bainite within ferrite
1	La	0.17/0.07	0.18/0.06	0.07/0.03	0.00/0.00
	Ce	0.24/0.09	0.10/0.04	0.00/0.00	0.01/0.00
2	La	0.00/0.00	0.19/0.08	0.00/0.00	0.00/0.00
	Ce	0.00/0.00	0.26/0.10	0.00/0.00	0.00/0.00
3	La	0.00/0.00	0.50/0.20	0.02/0.01	0.02/0.01
	Ce	0.00/0.00	0.45/0.17	0.05/0.02	0.00/0.00

The nucleation period τ for the formation of a new phase, such as proeutectoid ferrite or combined phases $\alpha + Fe_3C$, is inversely proportional to the nucleation rate J^* and the growth rate u, *i.e.*

$$\tau \propto (J^* \cdot u)^{-1} \quad \text{(1)}$$

J^* is proportional to the gross grain boundary energy, *i.e.* the product of A and σ, in which A is the gross boundary area and σ is the boundary energy per unit area. Referring to the nucleation theory in solid state transformation,[18)] J^* would be proportional to the square of the total driving force for transformation ΔG^2. The nucleation probability is supposed to be proportional to e^N where N is the ASTM No. for expressing the austenite grain size. J^* can be expressed as:

$$J^* \propto e^N \sigma \Delta G^2 \quad \text{(2)}$$

The growth rate of a new phase, u, can be expressed as:

$$u \propto \exp(-Q/RT) \quad \text{(3)}$$

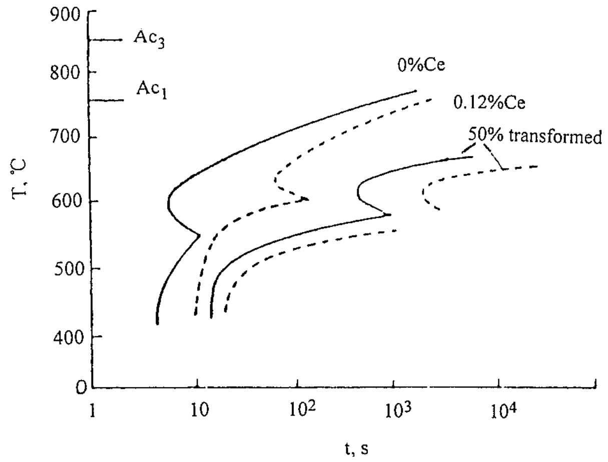

Fig. 3. Effect of Ce on the TTT diagram of a low carbon Mn–V–Ti steel, austenitized at 1 000°C.[15)]

Table 4. Chemical composition (wt%) and austenite grain size (ASTM No.) of steels 1 and 2 after austenitization at 1 000 and 1 100°C respectively,[15)] steels 3 and 4 after austenitization at 900°C for 10 min and 900°C for 120 min respectively,[17)] and steels 5, 6, 7 and 8 after austenitization at 900°C for 10 min.[12)]

Steel	C	Mn	Si	Ni	Cr	V	Ti	Al	S	P	Re	Grain size after austenitization at			
												1 000°C	1 100°C	900°C × 10 min	900°C × 120 min
1	0.11	2.10	0.27	0.27	0.27	0.077	0.014	0.022	0.01	0.011		7.5	~6.0		
2	0.11	2.12	0.28	0.26	0.31	0.085	0.027	0.041	0.002	0.007	0.12 (Ce)	7.5	~6.0		
3	0.27	0.65	0.86		1.23				0.012	0.009				9	6
4	0.28	0.65	0.86		1.10				0.010	0.007	0.17			10.5	9
5	0.20	1.02	0.14						0.015	0.033				6	
6	0.23	1.07	0.17						0.014	0.024	0.087			8	
7	0.25	1.12	0.20						0.014	0.041	0.16			8	
8	0.21	1.09	0.18						0.012	0.025	0.24			8	

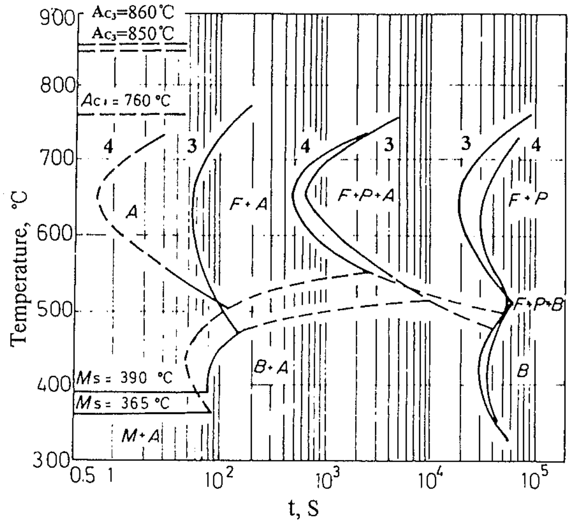

Fig. 4. Effect of RE on the TTT diagram of a 0.27C–1Cr steel.[17)]

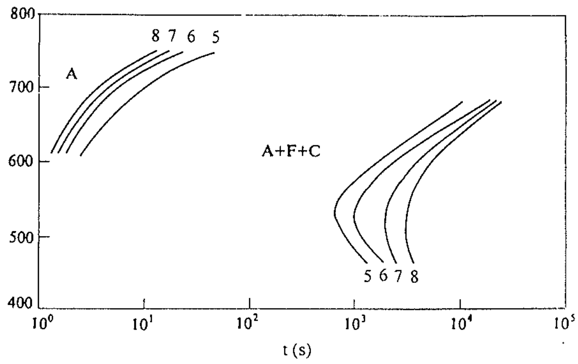

Fig. 5. Effect of RE on the TTT diagram of a 0.2C–1Mn steel.[12)]

where Q refers to the activation energy for growth and is related to the diffusion of carbon. Substituting Eqs. (2) and (3) into Eq. (1), we have

$$\tau = K\exp[\exp(N)A\sigma\Delta G^2\exp(-Q/RT)]^{-1} \quad \ldots.(4)$$

where K is a constant. Let τ_1 and τ_2 be the incubation period for steel free of RE and steel containing RE respectively. Then

$$\tau_1/\tau_2 = (K_1/K_2)\exp(N_2-N_1)(A_2/A_1)(\sigma_2/\sigma_1)(\Delta G_2/\Delta G_1)^2 \times\exp[(Q_1-Q_2)/RT] \quad \ldots\ldots(5)$$

in which the subscript number 1 refers to RE free steel and 2 to steel containing RE respectively. Suppose f be a function of N_1 and N_2 and

$$f(N_1, N_2) = K_1/K_2 = \begin{cases} N_1+N_2 & \text{when } |N_2-N_1| \geq 0.5 \\ 1 & \text{when } |N_2-N_1| < 0.5 \end{cases} \quad \ldots\ldots(6)$$

Let d_1 and d_2 be the average diameters of austenite grain and n_1 and n_2 be the number of austenite grain for RE free steel and steel containing RE respectively. For a specimen with the same volume V approximately, we have

$$V = n_1\pi d_1^3/6 = n_2\pi d_2^3/6 \quad \ldots\ldots(7)$$

$$n_2/n_1 = (d_1/d_2)^3 \quad \ldots\ldots(8)$$

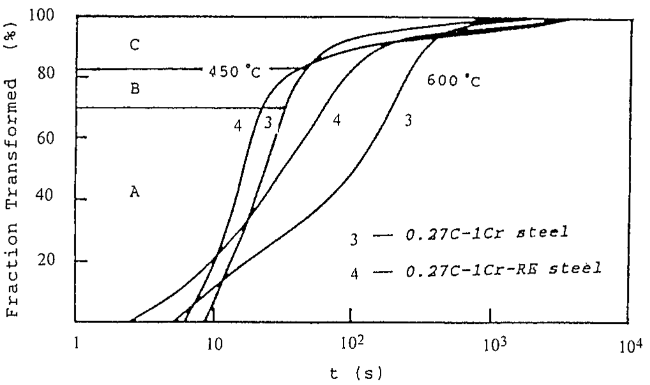

Fig. 6. Isothermal transformation curves at 600 and 450°C in steels 3 and 4.[19)]

and

$$A_2/A_1 = n_2\pi d_2^2/n_1\pi d_1^2 = d_1/d_2 \quad \ldots\ldots(9)$$

Substituting Eqs. (6) and (9) into Eq. (5), we have

$$\tau_1/\tau_2 = f(N_1, N_2)\exp(N_2-N_1)(d_1/d_2)(\sigma_2/\sigma_1)(\Delta G_2/\Delta G_1)^2 \times\exp[(Q_2-Q_1)/RT] \quad \ldots\ldots(10)$$

Equation (10) indicates the factors governing the hardenability of steel containing RE.

As for steels 1 and 2 (Fig. 3, Table 4), RE (Ce) mainly dissolves in the solid solution and segregates at the grain boundary of austenite and there is no marked change in grain size and carbon content of the austenite after the addition of Ce, *i.e.*, $N_1=N_2$, $d_1=d_2$, $\Delta G_1 \cong \Delta G_2$ and $\sigma_1>\sigma_2$. Consequently, RE (Ce) does enhance the hardenability of the steel, or $\tau_1/\tau_2<1$ and τ_1/τ_2 varies with the isothermal holding temperature as Q_1 and Q_2 are functions of the temperature, as shown in Fig. 3.

As for steels 3 and 4 (Fig. 4, Table 4), most of the RE content formed carbide and there shows the significant refinement of the austenite grain after the addition of RE. From Table 4, $N_1=9$ and $N_2=10.5$, $d_1=15.6\,\mu$m, $d_2=9.4\,\mu$m. The kinetics curves of the $\gamma\rightarrow$proeutectoid ferrite at the earlier stage of 600°C holding and the pearlitic transformation at the later stage of 600°C holding as well as the bainitic transformation at 450°C are shown in **Fig. 6**. The $\ln t$ ($y=0.5$) *vs.* $10^4/T$ curves of the proeutectoid ferrite formation in steels 3 and 4 are shown in **Fig. 7**, from which the activation energies $Q_1=29$ kJ/mol and $Q_2=46$ kJ/mol can be obtained.[19)] The relative grain boundary energies are $(\lambda_b/\lambda_s)_1=0.07$ and $(\lambda_b/\lambda_s)_2=0.38$,[20)] where λ_b is the free energy of grain boundary and λ_s is the surface energy. The ratio of grain boundary energy is approximately equal to that of the relative grain boundary energy, *i.e.*, $\lambda_2/\lambda_1=0.54$. The carbon contents in austensite of steel 3 is estimated as 0.104 wt% and that of steel 4, 0.063 wt% corresponding to the Ac$_3$ of 850°C in steel 3 and 860°C in steel 4 and the rest of carbon is considered to form carbides with high melting point which will not dissolve in solution at 900°C so that the carbon content in austenite at 900°C are 0.27 and 0.229 wt% respectively in steels 3 and 4. ΔG_1 and ΔG_2 can be calculated as $-1\,200$ and $-1\,300$ J/mol through the KRC model.[21)] The calculated incubation period ratio τ_1/τ_2 of the proeutectoid ferrite and the experimental ones at 700 and 650°C are in good agreement with each other, as shown in **Table 5**.

In steels 5–8 (Fig. 5, Table 4), by addition of RE, the more amount of carbide will be formed and the lesser carbon content will be in austenite at 900°C, accordingly the worse hardenability will be as shown in Fig. 5. The lattice parameters of martensite and proeutectoid ferrite of steels 5–8 (**Table 6**)12) verified the less carbon dissolved in solid solution with the increase of RE content. You *et al.*21) have also pointed out that RE lowers the amount of carbon, in participating the micro-diffusion in RE-containing steels.

The microstructure of proeutectoid ferrite in steel 1 (free of Ce) shows allotriomorph while that in steel 2 containing Ce is massive14) being consistent with the result obtained in steels 5–8 that the morphology of the proeutectoid ferrite changes from needle-like to equal-axis as RE content increases, as shown in **Fig. 8**.12)

Owing to the RE–carbide formation and the decrease of the carbon content in austenite as well as the refinement of the austenite grain, RE may shorten the incubation period of the proeutectoid ferrite formation, as shown in Fig. 5.

3. Effect of RE on the Pearlitic Transformation

Contradictory results of the effect of RE on pearlitic transformation have been reported. For example, RE may increase,16) decrease,22,23) or make no influence1) on the amount of pearlite formed after continuous cooling. Liu *et al.*12) and Lu *et al.*19) have studied the kinetics of isothermal pearlitic transformation and the morphology of pearlite formed after isothermal holding in steels containing RE compared with that in RE free steels.

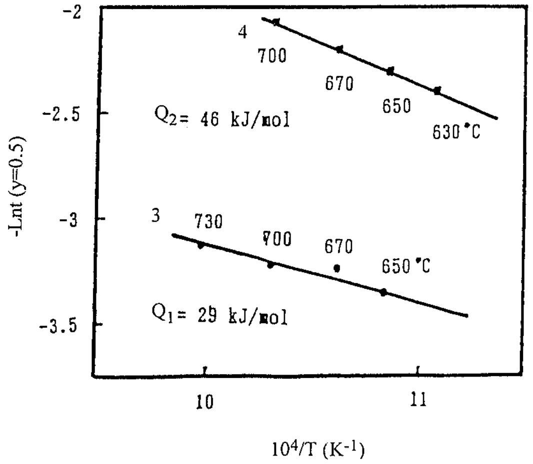

Fig. 7. $\ln t$ ($y=0.5$) *vs.* $10^4/T$ for proeutectoid ferrite formed isothermally in steels 3 and 4.19)

Following isothermal holding at 600°C to form 44% proeutectoid ferrite in steel 3 and 54% of that in steel 4, the pearlitic transformation occurs, and the transformation curves are shown in Fig. 6, indicating that RE retards the pearlitic transformation at later stages though it promotes the formation of the proeutectoid ferrite. It was reported that the nucleation rate of the proeutectoid ferrite in RE containing steel is 4-fold greater than that in RE free steel and the rate of the pearlitic transformation in RE containing steel, *i.e.*, steel 4, is only 2/3 of that in RE free steel, steel 3.19) The kinetics of the isothermal transformation in steels 5–8 (0.2C–1Mn series) gives similar results as shown in **Fig. 9**.12) The activation energy for the pearlitic transformation in steels 3 and 4 can be obtained from the $\ln t\,(y=0.5)$ *vs.* T^{-1} data as $Q_1=125$ kJ/mol and $Q_2=183$ kJ/mol, as shown in **Fig. 10**.19) The value of Q_1, 125 kJ/mol is close to the activation energy for carbon diffusion in austenite.25) The addition of RE increases the activation energy to 183 kJ/mole.

In steels 4, and 6, 7, 8, RE refines the austenite grain remarkably. Since the grain boundary is the preferential nucleation site for the proeutectoid ferrite, steels with

Table 5. Calculated and the experimental τ_1/τ_2 for proeutectoid ferrite formation in steels 3 and 4.17)

Temperature (°C)	τ_1 (sec), experimental	τ_2 (sec), experimental	τ_1/τ_2, experimental	τ_1/τ_2, calculated
700	7.5	1.4	5.36	6.67
650	5.5	0.8	6.88	6.12

Table 6. Influence of RE on the lattice parameter (nm) of martensite and proeutectoid ferrite in steels 5–8.12)

Steel	5	6	7	8
Martensite	0.28712	0.28730	0.28716	0.28716
Proeutectoid ferrite	0.28690	0.28690	0.28690	0.28690

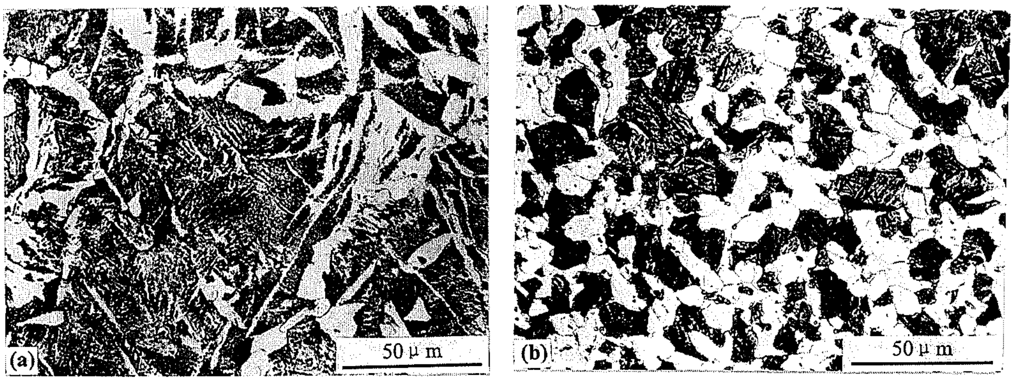

Fig. 8. Morphology of the proeutectoid ferrite isothermally formed at 700°C in steel 5 (a) (free of RE) and steel 8 (with 0.24% RE) (b).12)

refined austenite grain would obviously show high nucleation rate of the proeutectoid ferrite. Meanwhile, RE diminishes the diffusion coefficient of carbon and tends to segregate at the Fe_3C/α interface, hindering the growth of pearlite and increasing the activation energy for transformation. Consequently, RE may retard the rate of the pearlitic transformation at later stages as shown in Figs. 9 and 10.

It was found that RE decreases the amount of pearlite and affects the lamella spacing of the pearlite, *e.g.*, the average lamella spacing of the pearlite isothermally formed at 670°C in steels 3 and 4 are respectively 0.53 and 0.4 μm. **Figure 11** shows the scanning electron microstructures of the isothermally formed pearlite in steel 5(a) and 7(b), indicating that RE diminishes the lamella spacing of the pearlite.[12,19]

Let λ be the lamella spacing of pearlite and σ refer to the interfacial energy between cementite and ferrite and suppose that one third of the driving force for transformation, ΔG, will be consumed by the interfacial energy, then from thermodynamic derivation,[26,27] we have

$$\lambda = 6\sigma V/\Delta G \qquad (11)$$

where V is the molar volume of pearlite. Equation (11) indicates that lower interfacial energy will produce smaller lamella spacing of pearlite. As for steel 3, take $\sigma_1 = 0.7\ \mathrm{J/m^2}$,[26] we can get $\sigma_2 = 0.53\ \mathrm{J/m^2}$. The lowering of the interfacial energy between cementite and ferrite by addition of RE is considered to be caused by the segregation of RE at the interface, that is in good agreement with the experimental results, as shown in Table 2.

4. Effect of RE on the Bainitic Transformation

Han[28] reported that RE retards the bainitic reaction in steel. Lu *et al.*[17] and Lu *et al.*[29] studied the kinetics on bainite formation in a low carbon steel. The kinetics of the bainitic transformation at 450°C in steels 3 and 4 are shown in Fig. 6. The activation energy for bainitic transformation in steels 3 and 4 are obtained from **Fig. 12.**[29] In stage A of the bainite formation (in Fig. 6), the bainite mainly nucleate at the grain boundary of the austenite and the nucleation rate plays an important factor controlling the rate of transformation. As the addition of RE refines the austenite grain or increases the gross area of grain boundary, the nucleation rate of bainite in RE-containing steel (steel 4), N_2 will be much greater than in RE free steel (steel 3), N_1, the total transformation rate is so high as masking the retarding effect of RE on the transformation. Accordingly, at this stage, or at the very beginning of the bainite formation, the incubation period ratio obtained from Eq. (10) is $\tau_1/\tau_2 > 1$, as shown in **Table 7.**[17] In stage B, N_2 is slightly larger than N_1 and the growth rate of the new phase is a more important factor in the course of the transformation, so that the transformation rate in RE-containing steel (*i.e.* steel 4) is lower than that in RE free

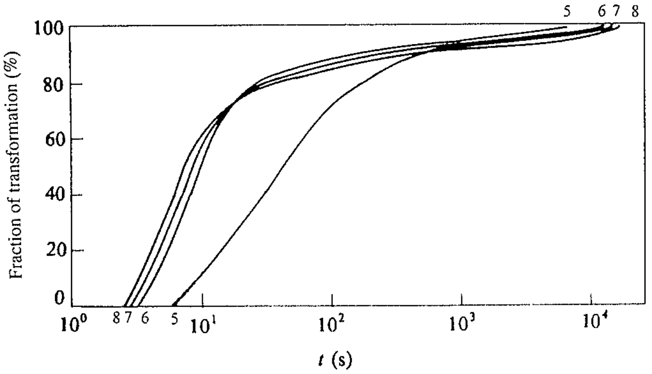

Fig. 9. Effect of RE on kinetics of the isothermal transformation at 670°C in steels 5–8 (0.2C–1Mn series).[12]

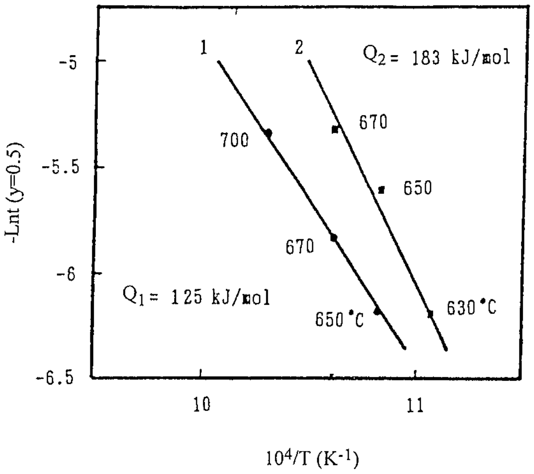

Fig. 10. ln t ($y=0.5$) *vs.* $10^4/T$ for pearlitic transformation in steels 3 and 4.[19]

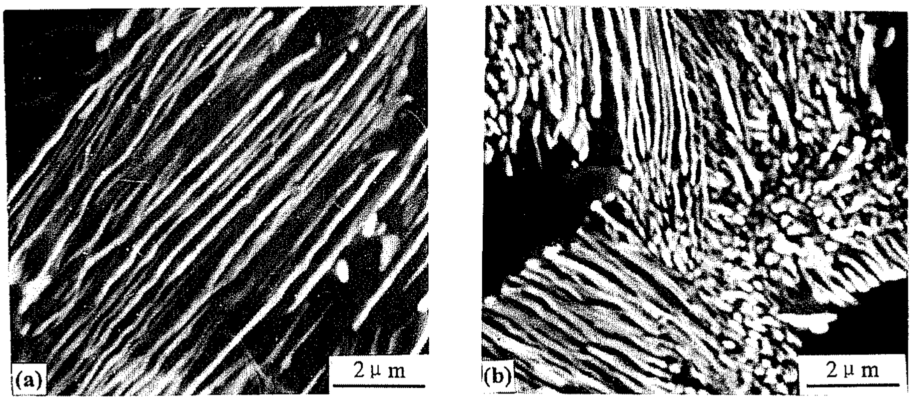

Fig. 11. Scanning electron micrograph of pearlite in steels 5(a) and 7(b).[12]

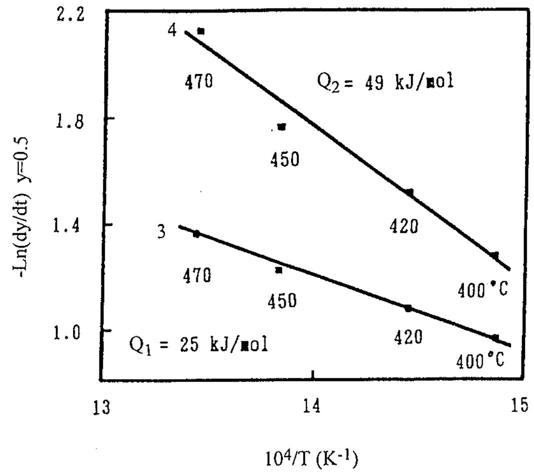

Fig. 12. $\ln(dy/dt)_{y=0.5}$ *vs.* $10^4/T$ in the course of bainite formation in steels 3 and 4.[29]

Table 7. Calculated and experimental incubation period ratio τ_1/τ_2 for bainite formation in steels 3 and 4.[17]

Temperature (°C)	τ_1 (sec), experimental	τ_2 (sec), experimental	τ_1/τ_2, experimental	τ_1/τ_2, calculated
550	7.2	3.5	2.1	4.45
450	12	5.5	2.2	1.18

steel (steel 3) owing to the dominant retarding effect of RE on transformation. In stage C as $f > 82\%$, there appears the stronger drag effect of RE on transformation and it may be attributed to the pinning of RE at ferrite/island interface (Table 3) and the lowering of diffusion coefficient of carbon by RE. At this stage, one may suppose $N_1 = N_2 = N =$constant and apply the Johnson–Mehl equation[30] to describe the kinetics and the drag effect of RE in the bainite reaction.

Define a drag factor α as the ratio of the growth rate in steel 4, G_2, and that in steel 3, G_1, *i.e.*,

$$\alpha = G_2/G_1 \quad \text{.........................(12)}$$

Thus, the smaller α is, the stronger the drag effect will be. From the Johnson–Mehl equation, we may have

$$\alpha = G_2/G_1 = (t_1/t_2)^{4/3} \quad \text{...................(13)}$$

For steels 3 and 4, substituting the data in Fig. 6 into Eq. (13), we can obtain the regression equation of α as

$$\alpha = (1\,034f^2 - 1\,757f + 718)^{-1} \quad \text{.............(14)}$$

where f is the transformation fraction. Eq. (14) can be shown as in **Fig. 13**.[29]

RE segregates at ferrite/island interface and produces the drag effect on growth. When the transformation proceeds, the gross area of island boundaries decreases and the relative segregation amount of RE per unit boundary area increases so that there appears a stronger drag effect resulting in the delay of the process of the bainite formation to completion.

Bainite in RE containing steels often appears as granular in morphology for RE segregation at boundary of ferrite/island, lowering the boundary energy.[29,31]

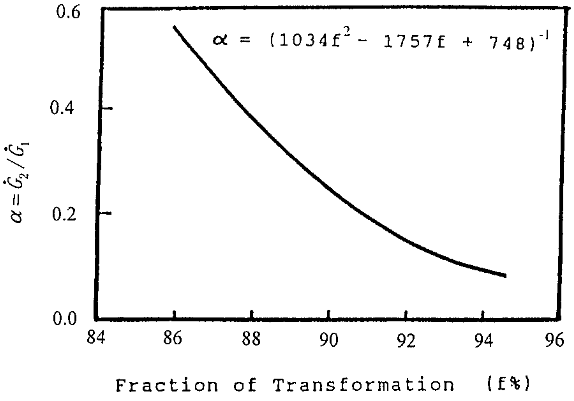

Fig. 13. Drag factor α in the course of bainite formation in steels 3 and 4.[29]

5. Effect of RE on the Lath Martensite Formation

Some previous works reported that the addition of RE to steel replaces twins with dislocations in lath martensite,[28,32] refines the size of lath martensite,[31,32] suppresses the autotempering in low carbon steel, but promotes the autotempering in a 0.4% carbon steel.[33] Hsu *et al.* studied the effect of RE on the lath martensite formation with respect to changes in M_s, substructure, autotempering ability, and the amount of retained austenite, as well as the distribution of RE in microstructure in the course of transformation.[34] In this article, the result from steels 3 and 4 in literature (34) are mainly reviewed.

The critical temperatures are $Ac_1 = 760$°C, $Ac_3 = 850$°C, $M_s = 390$°C in steel 3, and $Ac_1 = 760$°C, $Ac_3 = 860$°C, $M_s = 360$°C in steel 4 respectively. The slightly higher Ac_3 in steel 4 implies that there is less carbon content in austenite resulted from the formation of RE-carbides. The M_s temperature mentioned above is obtained by measurement of specimens of both steels quenched from 900°C for 10 min. The grain size of austenite is shown in Table 4. The lower carbon content in austenite in steel 4 must raise the M_s, yet the addition of RE will increase the required chemical driving force for martensitic transformation because of their strong affinity with carbon and lowering the activity coefficient of carbon in austenite and the increment of the non-chemical driving force needed for martensitic transformation by refining the austenite grain size from ASTM No. 9 to 10.5, *i.e.*, the strengthening of austenite. Thus, according to the thermodynamics of martensitic transformation of fcc(γ)→bcc(α) in Fe–C steels,[35–37] the addition of RE to steel may decrease the M_s, as from 390 to 365°C in steels 3 and 4.

The size of lath in RE containing steel is finer than in RE free steels, *e.g.*, the average lath thickness along [111] zone is 0.37 μm in the steel 3 and becomes 0.23 μm in the steel 4, as shown in **Fig. 14**. The amount of retained austenite existing as interlath martensitic films in the steel 4 is less than in the steel 3. Their greatest thicknesses of these films along the $[011]_\gamma$ zone are 9.7 and 27.8 nm in steels 4 and 3 respectively, as shown in **Figs. 15** and **16**, where exists the K–S relationship between austenite and martensite in both steels.[34]

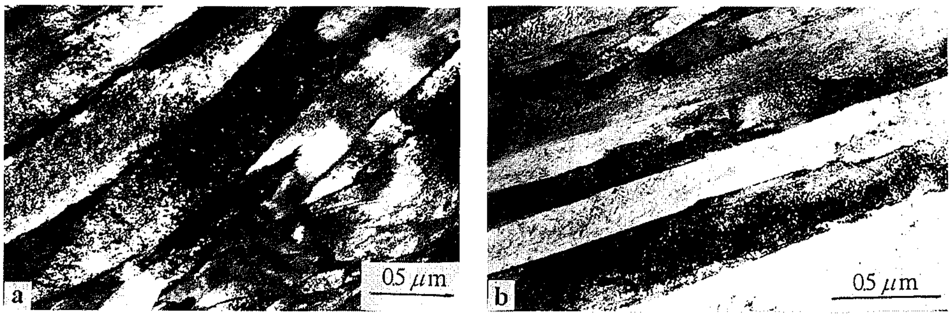

Fig. 14. Microstructure of lath martensite along its [111] zone in steel 3 (0.27C–1Cr steel) (a) and steel 4 (0.27C–1Cr–RE steel) (b).[34]

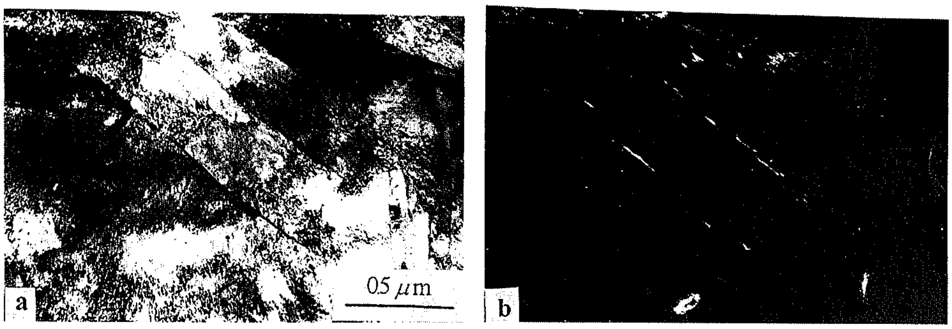

Fig. 15. Interlath films of retained austenite along its [011] zone in a quenched steel 4.[34]
(a) BF micrograph (b) DF micrograph.

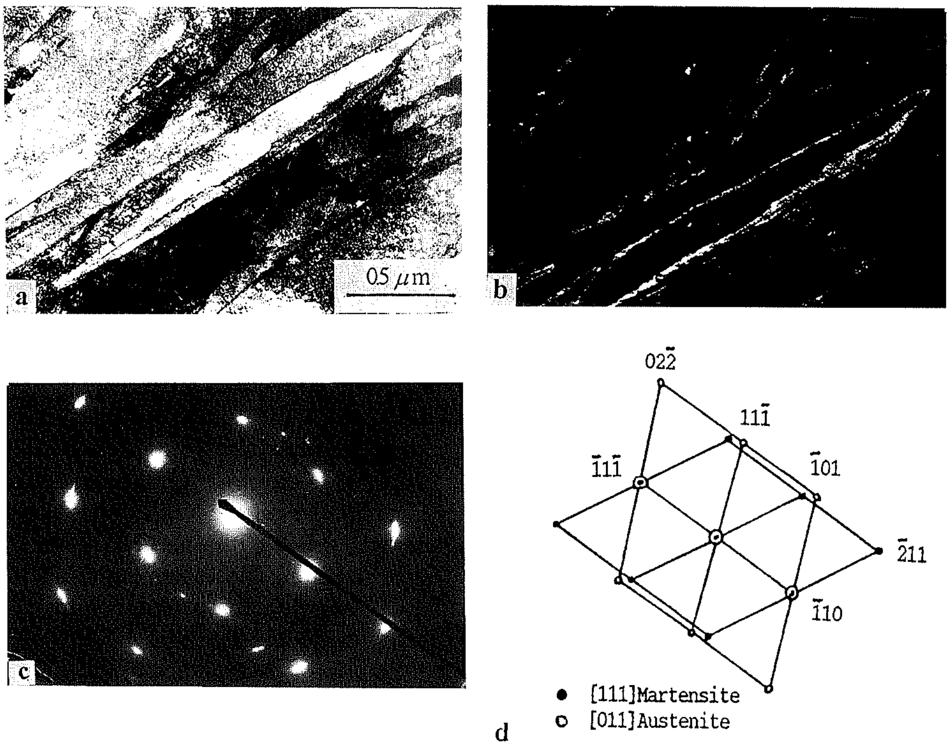

Fig. 16. Interlath films of retained austenite along its [011] zone in a quenched steel 3.[34]
(a) BF micrograph, (b) DF micrograph, (c) SAD pattern and (d) the corresponding indexed pattern.

It was found by EDAX[34] that in quenched steel 4 with 0.07 at% RE (or 0.17 wt% RE), the RE (La) segregates at prior austenite grain boundaries with an average composition of 0.191 at% as shown in **Fig. 17**, *i.e.*, the amount of RE is 4 times as much as that in martensite and retained austenite, and this kind of distribution will not change during the martensitic transformation. However, the segregation of RE at martensite/austenite interface cannot be detected where the average composition of 0.05 at% La is about the concentration in the solution of the bulk alloy. Although up to now, no experiment has shown in martensite(M)/austenite(γ) interface energy, it is reasonable to predict that RE will lower the M/γ interface energy which results in the formation of a thinner lath. Supposing the gross M/γ interface energy is equal for both steels, from the experimental thickness given above, the M/γ interface energy in RE-containing steel can be estimated as 0.6 of that in RE free steel.

There exists Fe_3C precipitation in both steels resulting from autotempering following martensitic transformation, as shown in **Figs. 18** and **19**. The size and density of Fe_3C precipitates in the steel 3 are both larger than those in the steel 4. The amount of Fe_3C precipitating during the martensitic transformation depends on (1) the carbon content in solution, (2) diffusion coefficient of carbon in martensite and (3) M_s temperature. These are all decreased by the RE addition so that autotempering is suppressed in the steel 4. Yao *et al.*[33] obtained the same result in an 0.2%C–Si–Mn–V steel, but reported that RE addition promoted autotempering in an 0.4%C–Si–Mn–V steel with an explanation that the amount of RE was insufficient to influence the carbon diffusivity. In their work, the ASTM No. of austenite and M_s data were not given, and probably the RE addition did not refine the austenite grain size, but raised the M_s temperature, resulting in a greater extent of autotempering.

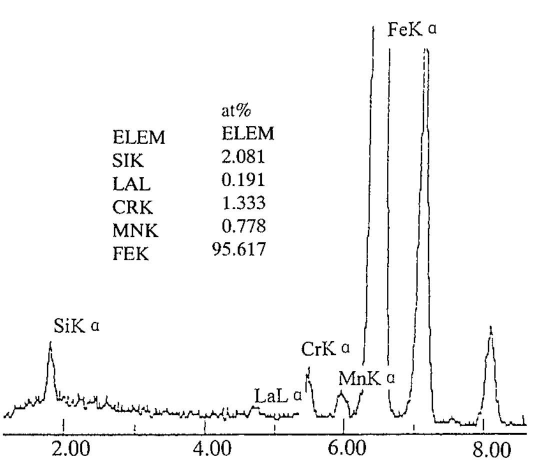

Fig. 17. Segregation of La at the prior grain boundary of austenite in steel 4 (0.27C–1Cr–RE).[34]

From Figs. 14–16, it can be seen that there is less retained austenite in steel containing-RE, although RE addition will lower the M_s. Magee[38] derived an equation describing the volume fraction of retained austenite in quenched steels as

$$\gamma = \exp[-\bar{V}\varphi(d\Delta G^{\gamma\to\alpha}/dT)(M_s - T_q)] \quad \text{........(15)}$$

where T_q is the quenching medium temperature, $\bar{V}$ is the average volume of the newly formed martensite plate, $\Delta G^{\gamma\to\alpha}$ is the difference in free energy per unit volume between austenite and martensite, and φ is a proportionality constant. The $\bar{V}$ and $d\Delta G^{\gamma\to\alpha}/dT$ are assumed to be constants. Koistinen and Marburger[39] obtained an empirical equation for 0.37–1.10 wt% C steels from experiment as

$$\gamma = \exp[-1.10\times 10^{-2}(M_s - T_q)] \quad \text{..........(16)}$$

It is apparent from Eqs. (15) and (16) that more austenite will be retained at lower M_s for a given value of T_q. Equation (15) is generally in good agreement with experimental results in steels containing >0.3 wt% carbon. However, this principle is unavailable for low carbon steel, especially when the low carbon steel contains alloying elements lowering the activity of carbon, as the rare earth element. Both theory[40–42] and experiment[41,43,44] make it clear that there exists carbon diffusion during martensitic transformation in low carbon steels. Therefore, the general equation describing

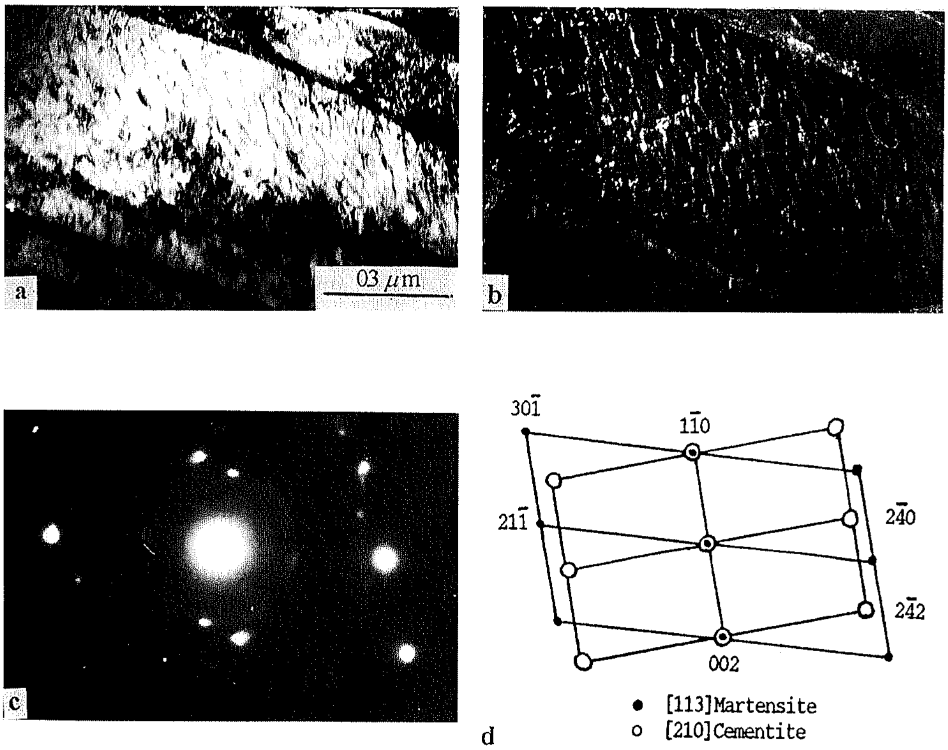

Fig. 18. Fe_3C precipitates formed during autotempering in steel 3.[34] (a) BF micrograph, (b) DF micrograph, (c) SAD pattern and (d) the corresponding indexed pattern.

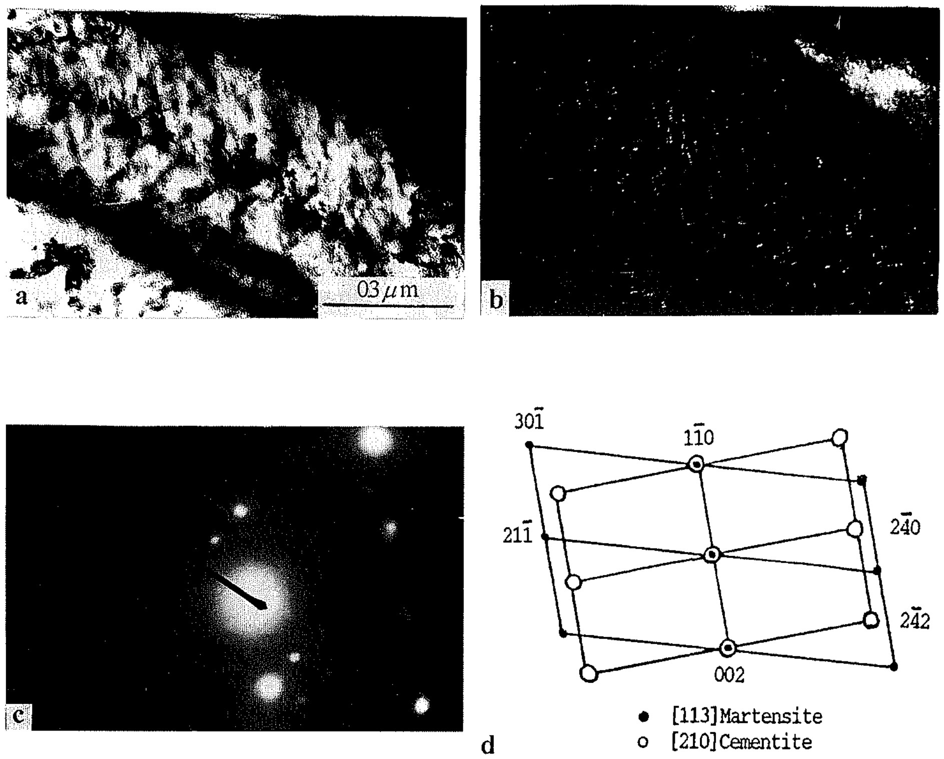

Fig. 19. Fe_3C precipitates formed during autotempering in steel 4.[34] (a) BF micrograph, (b) DF micrograph, (c) SAD pattern and (d) the corresponding indexed pattern.

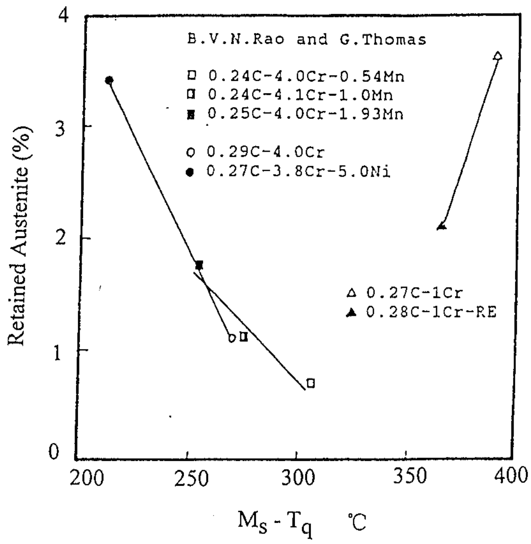

Fig. 20. The volume fraction of retained austenite *vs.* (M_s-T_q) in some low carbon steels.[34]

the retained austenite amount must show the influence of carbon diffusion on the $\Delta G^{\gamma\to\alpha}$. In low carbon steel, *e.g.* C < 0.27 wt%, the $\Delta G^{\gamma\to\alpha}$ is a function of temperature and the carbon content in steel. Referencing the Magee's derivation, the $d\Delta G^{\gamma\to\alpha}$ ought to be expressed as

$$d\Delta G^{\gamma\to\alpha}=(\partial\Delta G^{\gamma\to\alpha}/\partial T)dT+(\partial\Delta G^{\gamma\to\alpha}/\partial c)dc \quad ....(17)$$

in which c stands for the carbon concentration. The $\partial\Delta G^{\gamma\to\alpha}/\partial T>0$ and $\partial\Delta G^{\gamma\to\alpha}/\partial c>0$ because the $\Delta G^{\gamma\to\alpha}$ decreases more negative as the T or c decreases. Assuming $\partial\Delta G^{\gamma\to\alpha}/\partial T$ and $\partial\Delta G^{\gamma\to\alpha}/\partial c$ be constant, integrating T from M_s to T_q and c from c_0 to c_1 where c_0 and c_1 are the carbon contents of austenite at the onset and end of martensitic transformation respectively, we have

$$\gamma=\exp \bar{V}\varphi[\partial\Delta G^{\gamma\to\alpha}/\partial c(c_1-c_0)-\partial\Delta G^{\gamma\to\alpha}/\partial T(M_s-T_q)]$$

or

$$\gamma=\exp[\alpha(c_1-c_0)-\beta(M_s-T_q)] \quad ....(18)$$

where $\alpha=\bar{V}\varphi\partial\Delta G^{\gamma\to\alpha}/\partial c$, and, $\beta=\bar{V}\varphi\partial\Delta G^{\gamma\to\alpha}/\partial T$.

In **Fig. 20**, the volume fraction of the retained austenite is plotted against the temperature difference between M_s and T_q in degrees centigrade for the steels 3 and 4 and the low carbon steels containing Mn and Ni from Rao and Thomas's work.[45] The addition of Mn in steel does not change the c_1 because Mn has very small effect on the carbon diffusion. The higher amount of retained austenite is only due to the lower M_s caused by the solution strengthening from the addition of Mn.[47,48] Ni raises the activity of carbon in austenite so as to increase the c_1 and therefore more austenite will be retained. Addition of RE strongly lowers the activity coefficient of carbon in austenite, in turn, lowers the c_1 so as to greatly reduce the amount of retained austenite, although the lowering of M_s will slightly increase the amount of the retained austenite. In medium and high carbon steels, there does not occur the carbon diffusion during the martensitic transformation, so $c_1=c_0$ and therefore the general equation (18) will be reduced to Magee's equation, *i.e.* Eq. (15). The Eq. (18) can be used for all steels and reveals the influence of alloying elements which would increase or decrease the activity coefficient of carbon on the amount of retained austenite after quenching, *i.e.*, Ni and Si increase the retained austenite, and RE, V and Mo may have reverse effect.[49] The amount of the retained austenite is closely related to the toughness of low carbon steel[45] and is a significant factor for modern steel design.[50]

6. Conclusions

(1) Rare earth elements (RE) may segregate at the grain boundaries of austenite, tend to form carbide (in turn may decrease the carbon content in solution) and refine the austenite grain.

In case of RE segregation at grain boundaries of austenite and unalteration of the grain size as well as the carbon content of austenite, addition of RE to steel would increase the hardenability of steel. In case of a domination of grain refinement by RE addition, RE will deteriorate the hardenability.

The incubation period of the proeutectoid ferrite can be expressed as a function of grain boundary energy, grain size, activation energy for growth and ΔG for the proeutectoid ferrite formation, and the calculated results τ_1/τ_2 at 700 and 650°C for 0.27C–1Cr and 0.27C–1Cr–RE steels are in good agreement with the experimental data.

RE will replace the allotriomorph proeutectoid ferrite into massive ferrite.

(2) RE may retard the isothermal pearlitic transformation, *e.g.*, the transformation rate in 0.27C–1Cr–RE steel is only 2/3 of that in 0.27C–1Cr steel and the activation energies of the transformation are 185 and 125 kJ/mol respectively because RE diminishes the diffusion coefficient of carbon as well as tends to segregate at Fe_3C/α interface showing a pinning effect on the transformation.

RE may reduce the lamella space of the pearlite and lower the Fe_3C/α interfacial energy, for example, addition La to a 0.27C–1Cr steel lowers the interfacial energy from 0.7 to 0.53 J/m^2 estimated from the lowering lamella space from 0.53 to 0.4 μm in pearlite formed at 670°C.

(3) Granular bainite forms in RE-containing steel and RE tends to segregate at ferrite/island interface. Kinetics of the isothermal bainitic transformation in refined austenite grain steel with addition of RE shows that at the earlier stage the transformation rate is high, while at the later stage it becomes sluggish. The activation energy for the bainitic reaction increases from $Q_1 = 23$ kJ/mol in a 0.27C–1Cr steel to $Q_2 = 49$ kJ/mol in 0.27C–1Cr–RE steel. The segregation of RE at ferrite/island interface may act as a drag effect. As a drag factor α is defined as a ratio of the growth rates in RE-containing and RE free steels. α is a function of the transformation fraction f and it decreases with f.

(4) RE segregates at the grain boundary of austenite and this kind of distribution will not change during the martensitic transformation. However, no experiment has shown the martensite/austenite interface energy, it is reasonable to predict that RE will lower the energy which results in the formation of a finer lath martensite.

(5) RE lowers M_s but decreases the amount of the retained austenite. RE retards the autotempering process. It is emphasized that the amount of the retained austenite, γ, in quenched low carbon steel depends on not only the M_s and the temperature of quenching medium but also the influence of alloying elements on the carbon diffusion during quenching. A general equation describing the extent of the austenite–martensite transformation is suggested as

$$\gamma = \exp[\alpha(c_1 - c_0) - \beta(M_s - T_q)]$$

where c_0 and c_1 are carbon concentrations in austenite before and after quenching respectively, α and β are constants related to materials. RE decreases M_s, but also lowers c_1 so as to reduce the amount of the retained austenite.

REFERENCES

1) Z. Yu, Y. Chou, X. He, G. Du, P. Gao and F. Zhu: Rare Earth in Steel, Metallurgical Industrial Press, Beijing (in Chinese), (1982), 127.
2) J. Yu, Z. Yu and C. Wu: *Chin. J. Met. Sci. Technol.*, **5** (1989), 33.
3) S. Zhang and C. Wu: Proc. 3rd Int. Congress on Heat Treatment of Materials, Vol. 3, (1983), 15.
4) Q. Han, W. Wu, K. Fang, C. Hue and X. Zhou: *Iron Steel (China)*, **17** (1982), No. 2, 1 (in Chinese).
5) K. Fang and R. Ni: *Metall. Trans.*, **17A** (1986), 315.
6) Y. Yang: *Trans. Met. Heat Treat. (China)*, **2** (1981), No. 1, 8 (in Chinese).
7) J. Qiu: Application of Rare Earth in Iron and Steel (in Chinese), Metallurgical Industrial Press, Beijing, (1987), 251.
8) D. Zhang and C. Wu: *Acta Metall. Sin. (Engl. Ed.) A*, **1** (1988), 113.
9) D. Zhang, C. Wu and R. Yang: *Mater. Sci. Eng.*, **A131** (1991), 93.
10) W. Lu, H. Liu and T. Y. Hsu (Xu Zuyao): *Scr. Metall. Mater.*, **29** (1993), 273.
11) W. Lu, H. Liu and T. Y. Hsu (Xu Zuyao): *Iron Steel (China)*, **29** (1994), No. 4, 43 (in Chinese).
12) H. Liu, D. Zheng and T. Y. Hsu (Xu Zuyao): *J. Rare Earth*, **10** (1992), No. 3, 189.
13) A. P. Guliaev, E. A. Ulianin, Mu TOM, (1963), No. 8, 2.
14) X. He, Y. Chu, X. Zhang, Z. Yu, Q. Li and X. Ying: *Acta Metall. Sin. (China)*, **13** (1977), 235 (in Chinese).
15) C. Wu and B. Zhang: *J. Chin. Soc. Rare Earth*, **10** (1992), No. 1, 48 (in Chinese).
16) Z. Liu, W. Li and C. Li: *Trans. Met. Heat Treat. (China)*, **11** (1990), No. 1, 75 (in Chinese).
17) W. Lu, D. Zheng and T. Y. Hsu (Xu Zuyao): *Acta Metall. Sin. (China)*, **29** (1993), A307 (in Chinese).
18) T. Y. Hsu (Xu Zuyao): Theory of Phase Transformation, Science Press, Beijing (in Chinese), (1988), (1991), 176.
19) W. Lu, L. Zhang and T. Y. Hsu (Xu Zuyao): *Iron Steel (China)*, **28** (1993), No. 9, 62 (in Chinese).
20) V. N. Gurashchev and N. I. Maiorov: *Liteinoe Proizvod.* (Foundry Production) (in Russian), (1972), No. 5, 1.
21) T. Y. Hsu (Xu Zuyao) and Y. W. Mou: *Acta Metall.*, **32** (1984), 1469.
22) M. You, J. Yang and D. Chen: Application of Rare Earth in Iron and Steel (in Chinese), Metallurgical Industrial press, Beijing, (1987), 268.
23) Y. Liu and R. Gao: *Rare Earth*, (1987), No. 4, 19 (in Chinese).
24) Q. Lin, W. Ye, S. Li and Z. Yu: *J. Chin. Soc. Rare Earth*, **8** (1990), No. 1, 52 (in Chinese).
25) C. Wells and R. F. Mehl: *Met. Technol.*, **7** (1940), No. 5, 1.
26) J. J. Kramer, G. M. Pound and R. F. Mehl: *Acta Metall.*, **6** (1958), 763.
27) T. Y. Hsu (Xu Zuyao): Thermodynamics of Metallic Materials, Science Press, Beijing (in Chinese), (1981), (1983), 280.
28) Y. Han: Application of Rare Earth in Iron and Steel (in Chinese), Metallurgical Industrial Press, (1987), 275.
29) W. Lu, L. Sun and T. Y. Hsu (Xu Zuyao): *Iron Steel (China)*, **29** (1994), No. 11, 44 (in Chinese).
30) W. A. Johnson and R. F. Mehl: *Trans. AIME*, **135** (1939), 416.

31) H. Liu, D. Zheng and T. Y. Hsu (Xu Zuyao): *Ordnance Mater. Sci. Eng.*, **15** (1992), No. 1, 77 (in Chinese).
32) Y. Huang: *Ordnance Mater. Sci. Eng.*, **11** (1988), No. 8, 8 (in Chinese).
33) Y. Yao, T. Zhou and X. Wang: *Trans. Met. Heat Treat. (China)*, **12** (1991), No. 2, 8 (in Chinese).
34) T. Y. Hsu (Xu Zuyao), W. Lu and Y. Wang: *Iron Steel (China)*, **30** (1995), No. 4, 52 (in Chinese).
35) T. Y. Hsu (Xu Zuyao): *Acta Metall. Sin. (China)*, **16** (1980), 426 (in Chinese).
36) T. Y. Hsu (Xu Zuyao): *J. Mater. Sci.*, **20** (1985), 23.
37) T. Y. Hsu (Xu Zuyao): Proc. ICOMAT-86, Keynote Lecture, The Jap. Inst. Met., (1987), 245.
38) C. L. Magee: Phase Transformations, ASM, (1970), 115.
39) D. P. Koistinen and R. E. Marburger: *Acta Metall.*, **17** (1959), 59.
40) T. Y. Hsu (Xu Zuyao) and X. M. Li: *Scr. Metall.*, **17** (1983), 1285.
41) T. Y. Hsu (Xu Zuyao) and X. Li: *Acta Metall. Sin. (China)*, **19** (1983), A83 (in Chinese).
42) T. Y. Hsu (Xu Zuyao) and X. Li: *Acta Metall. Sin. (China)*, **19** (1983), A505 (in Chinese).
43) B. V. N. Rao and G. Thomas: Proc. ICOMAT-79, MIT, USA, (1979), 12.
44) M. Sarikaya, G. Thomas, J. W. Steeds, S. J. Barnard and D. W. Smith: Proc. Int. Conf. Solid-Solid Phase Transformation, ed. by A. I. Aaronson *et al.*, TMS-AIME, (1982), 1421.
45) B. V. Rao and G. Thomas: *Metall. Trans.*, **11A** (1980), 441.
46) H. B. Chang and T. Y. Hsu (Xu Zuyao): *Acta Metall.*, **34** (1986), 333.
47) T. Y. Hsu (Xu Zuyao) and M. Pan: *Acta Metall. Sin. (Engl. Ed.)*, **3A** (1990), 16.
48) M. Pan and T. Y. Hsu (Xu Zuyao): *Acta Metall. Sin. (Engl. Ed.)*, **3A** (1990), 153.
49) T. Y. Hsu: *J. Phys.*, Colloque C8, Suppl. III, 5 (1995), C8-351.
50) T. Y. Hsu (Xu Zuyao): *Shanghai Met.*, **17** (1995), No. 1, 1 (in Chinese).